MgO/Ag(001) interface structure and STM images from first principles

N. Lopez[1] and S. Valeri[2]
[1]*Dept. Quimica Fisica and Centre Especial de Recerca en Quimica Teorica, Universitat de Barcelona and Parc Cientific, c/Marti i Franques 1, E-08028 Barcelona, Spain*
[2]*INFM-National Research Center on Nanostructures and Biosystems at surfaces* (S^3)*, Via Campi 213/a, 41100 Modena, Italy*
(Received 24 December 2003; revised manuscript received 25 June 2004; published 29 September 2004)

The interface of MgO/Ag(001) has been studied with density functional theory applied to slabs. We have found that regular MgO films show a small adhesion to the silver substrate, the binding can be increased in off-stoichiometric regimes, either by the presence of O vacancies at the oxide film or by a small excess of O atoms at the interface between the ceramic to the metal. By means of theoretical methods, the scanning tunneling microscopy signatures of these films is also analyzed in some detail. For defect free deposits containing 1 or 2 ML and at low voltages, tunnelling takes place from the surface Ag substrate, and at large positive voltages Mg atoms are imaged. If defects, oxygen vacancies, are present on the surface of the oxide they introduce much easier channels for tunnelling resulting in big protrusions and controlling the shape of the image, the extra O stored at the interface can also be detected for very thin films.

DOI: 10.1103/PhysRevB.70.125428 PACS number(s): 68.55.−a, 68.35.Ct, 68.37.Ef, 71.15.Mb

I. INTRODUCTION

The metal/oxide interface is of interest due to the very large number of applications in several fields of technological application. So far, most of the studies have been applied to the investigation of the systems where oxides act as supports for metals; this is mainly because these structures are at the core of the performance of most of the industrial catalytic materials.[1–3] A second aspect of the research on metal oxide interface, this is the growth of oxides on metals, is mostly relevant to the formation of anticorrosion protections or thermal and electric insulators.[4] However, the chemical properties of these "reverse" catalysts, have also attracted significant attention.[5]

The interest of the oxide on metal systems goes even further since a large number of oxides are insulators and, in order to explode the powerful ultra-high vacuum techniques, it is needed to prepare them as ultra thin films on conductive supports, i.e. metals.[1,6,7] A larger flexibility is obtained by growing oxides on metals since it is possible that the oxides inherit, to a certain extent, some of the properties of the metal, in particular geometries, stabilizing new structures not present in the bulk or the surface of clean oxides. A detailed description of these ultra thin films is still lacking. A first investigation on the properties of Al_2O_3 on NiAl was performed by Jennison and co.,[8] and recently vanadium oxides on Pd(111) have been studied in the submonolayer regime.[5] Yet, other important points, already suggested for the MgO/Ag(001) system, are the dependence of the insulator character with the thickness of the thin film and the possibility of high reactivity of these deposits towards water.[9–12]

The Ag/MgO interface has been, for a long time, a playground for the metal to oxide interaction,[13,14] this is due to the very small mismatch between the two lattices, around 3%. The same reason explains why the reversed system (MgO on Ag) has been chosen to deeply investigate the properties at the oxide/metal interface. The simplicity of this system has given rise to several experimental and theoretical studies. The most powerful tool to analyze structural aspects of conductive surfaces is scanning tunnelling microscopy (STM) that allows a careful geometric characterization up to atomic resolution. Schintke and co.[9] have reported the first STM images and the corresponding spectroscopy, STS, investigation complemented by some calculations on the MgO/Ag(001) system. They have shown the evolution of the insulator character with oxide thickness and they have achieved atomic resolution on the MgO film suggesting the origin of the contrast observed in the images. As for the theoretical side, some of the earlier results published on the system were an application of the Harris Functional that demonstrated the relevance on impurities in adhesion.[15] Pisani and co.[16] have reported adhesion energies and parameters at the MgO/Ag interface for regular stoichiometric deposits. They have also investigated the origin of the reactivity towards H_2O. More recently, these authors have extended their investigation to the isostructural NiO/Ag(001)[17] system.

Our aim in the present paper is to obtain the energetics of oxide adhesion to the metal and characterize the structure at the interface. In particular, investigating how geometries and energies can be affected by the excess or the deficit of oxygen during the growing process. The final step is to give hints through the simulation of STM images for a detailed characterization of these deposits.

II. COMPUTATIONAL DETAILS

We have employed the density functional theory, DFT, as implemented in the Dacapo code,[18] applied to slabs representing the MgO/Ag(001) interface to determine the geometries, energies, electronic structure of this interface and to simulate the STM images. Calculations employ ultra soft pseudopotentials[19] to describe the ionic cores while the Kohn-Sham one-electron valence states are expanded in a basis of plane waves with kinetic energies below 340 eV.

The employed Monkhorst-Pack mesh is $8\times8\times1$ for the MgO(001)/Ag(001) interface, and has been reduced accordingly when enlarging the cell. The exchange-correlation energy is described by the generalized gradient approximation PW91.[20] The self-consistent PW91 density is determined by iterative diagonalization of the Kohn-Sham Hamiltonian. Fermi population of the KS states (k_BT=0.2 eV) and Pulay mixing of the resulting electronic density[21] have been used.

To represent the metallic substrate three layers of Ag(001) have been employed where only the first one has been allowed to relax. On top of it one or two layers of MgO(001) have been deposited, where the O atoms are on top of the Ag centers[22] and compressing the Mg-O distance so as to fit the cell of Ag (this is about 3%). When modeling defective surfaces a $p(2\times2)$ supercell is used, leading to a 0.25 ML in plane coverage of neutral vacancies or excess O atoms. For O-deficient systems calculations have been performed for a single vacancy in the topmost layer and at the interface when 2 ML of MgO exist. In fact, a 15% O deficit on the MgO samples has been reported for some of the experiments.[23] To complete the investigation of the role of the O_2 ambient we have explored the excess oxygen at the interface between the metal and the MgO film. Subsurface oxygen atoms have been placed between the metal and the oxide; the resulting MgO/O/Ag structure has been analyzed only for a single MgO layer on top of the partially O-covered Ag surface. For O_2 on Ag(111) it has been found that only the initial 0.25 ML O-atoms are staying on the surface of Ag and as the coverage increases a certain amount of oxygen will sit in subsurface sites, almost 50% for 1 ML coverage.[24] A similar behavior for the Ag(001) surface is expected. Again in this case, a $p(2\times2)$ unit cell has been employed to show a coverage of interstitial O atoms of 0.25 ML. The notation employed through the paper is the following: V states for oxygen vacancies, that can be either on the surface for which an "s" subindex is employed or at the interface represented by an "i" label. When preoxidized silver exists, the pre-existent O layer is also described as interface "i" and the first MgO layer is considered as a surface "s" layer. Schematic representation for the systems employed in the calculation can be found in Fig. 1.

To simulate the STM images we have employed the Tersoff-Hamann approach[25] that simplifies the tunnelling probability by imposing finite temperature and a point representation of the tip located at **r**. According to their approach, shown in Eq. (1), the general expression for the tunnel intensity can be approximated by:

$$I\alpha\Sigma_\mu \int |\phi_\mu(\mathbf{r})|^2\omega(\epsilon)d\epsilon, \tag{1}$$

where I is the tunnelling intensity, $|\phi_\mu(\mathbf{r})|^2$ is the density of state μ at a certain position and $\omega(\epsilon)$ is the weight function that determines the contribution from different states available for tunnelling. For zero bias $\omega(\epsilon)$ is replaced by a Gaussian function and the intensity turns out to be proportional to the density of states at the Fermi level at the tip position.

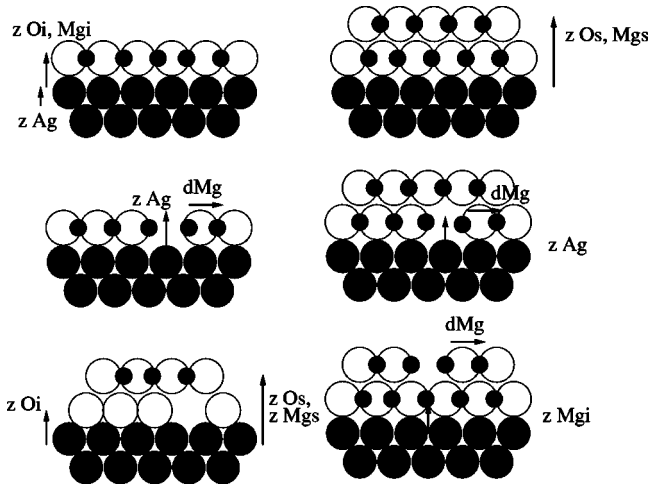

FIG. 1. Schematic representation for the studied systems. Top panel regular MgO on Ag (001): left 1 ML, right 2 ML. Central defective structures when defects are localized at the interface. Lower panel, left a single MgO layer on partially preoxidized Ag and right 2 ML of MgO adsorbed on Ag(001) with a defect on the surface layer. Black spheres correspond to Ag atoms, white corresponds to O anions and small black spheres represent Mg cations. The arrows indicate relevant positions or displacements reported in Tables I and II.

The presence of a finite bias introduces more states available for the tunnelling process. When the sample is biased positively electrons flow from the tip to the sample and there is a continuum of states; those with energies between the Fermi level and the value of the positive bias, available for the tunnelling processes. In the Tersoff-Hamann formalism such a contribution can be introduced by the weight function, $\omega(\epsilon)$, a window-like function containing all the states coming from the sample and located between the Fermi energy and the voltage applied. In this case, we have taken it to be the difference between the two Fermi functions, corresponding to the sample and to the tip, respectively.

Voltages employed in the simulations are on the order of those employed experimentally; this is from 0 to 3 V.[26] Typical values selected for the constant density at which the images are obtained: for zero bias are 4×10^{-4} e/Å^3 while for a voltage of 3 V the density value was increased to 2×10^{-3} e/Å^3. These values chosen so they provide better agreement with the corrugation observed in the experiments. In that way the represented image corresponds to a constant current mode instead of a constant tip-substrate separation. A similar approach has been successfully applied to the study of TiO_2(110).[27–29]

Other approaches, that explicitly calculate the coupling between the wavefunctions of the tip and the sample, have been proposed. However, they are more complicated and have mostly been applied to wavefunctions calculated through the Extended-Hückel approximation.[30] Due to the complexity of the oxide/metal interface, the Extended-Hückel approximation might not be the best choice when describing this system.

TABLE I. Geometries for $L=1$ and 2 ML of MgO on the Ag(001) surface. *i* stands for the layer in contact with the metal while *s* stands for the surface oxide layer. Distances are in Å.

L	z_{Ag}	z_{Oi}	z_{Mgi}	z_{Os}	z_{Mgs}
1	−0.027	2.546	2.455	-	-
2	−0.055	2.472	2.446	4.644	4.607

III. RESULTS

The results are presented as follows. First, we have investigated the geometry and structure at the oxide/metal interface with different O_2 contents. In a second step, we have analyzed the energetics for oxide adhesion, showing which are the most stable structures; and finally we have obtained the corresponding simulated STM images at different voltages giving clues to monitor and assign the features already observed experimentally in the images.

A. Geometry at the interface

We start by analyzing the geometry of the different structures calculated. In all cases, the anions of the MgO film directly in contact with the metal have been located on top of the metal atoms as suggested from previous calculations.[9,16,22]

For a single oxide layer the geometries are in very good agreement with previous results.[16] A single layer of MgO adsorbed on Ag(001) presents a significant corrugation, almost 0.1 Å. The overlayer-substrate interfacial distance for Mg and O, 2.46 Å and 2.55 Å, respectively. Corrugation alleviates the geometrical constraints induced by the support, releasing some of the energy introduced by film compression to accomodate the Ag(001) cell parameter. The relative distance along the *z*-direction between anions and cations is reduced for the bilayer compared to that of the monolayer. Only a 0.03 Å difference between the positions of surface anions and the cations has been evaluated; see Table I. However, the tetragonal distortion induced by the misfit at the interface is seen in the whole oxide structure. The average distance between the first and the second layer of the supported bilayer of MgO is elongated with respect to that of bulk MgO by 3%, an elongation of 3.6% has been reported experimentally for 3 ML MgO films, and a complete recovering of the bulk value has been observed for 6 ML.[23,33] More detailed measures for the oxide to metal distances are also available from different experiments. The interface distance MgO to Ag has been found to be 2.43±0.02 by EXAFS,[32] 2.53±0.05 by GIXRD[14] and 2.39±0.06 Å by LEED.[31] The latter authors also provide the values found in their calculations. They reported a distance of 2.39–2.55 Å for the monolayer and 2.46–2.55 Å for the bilayer with a second layer of atoms placed at 4.65 Å. This is rather similar to the values we have computed, especially taking into account that a more extensive optimization has been performed in the present case.

We have computed different off-stoichiometric MgO/Ag structures in a $p(2\times2)$ configuration; see Table II. If silver is preoxidized, subsurface oxygen atoms are sitting at the hollow sites of the Ag(001) structure. It has been seen experimentally that O atoms are above the hollow site at about 0.6 Å out of the Ag surface.[34] This value is rather similar to our estimate, 0.5 Å for the O adsorbed on Ag(001) for the MgO/O/Ag system. When MgO is deposited on top of the preoxidized structure the presence of the interstitial O gives rise to a larger distance from the surface metal atoms to both anions and cations of the MgO layer. The corrugation is smaller than in previous cases. The distances from Ag surface atoms are about 2.73 Å for O and for Mg not in contact with the interface O_i; see Table II. These Mg cations are found from 0.3 Å lower; this can have implications in the simulated STM images. It is important to notice that the distances observed experimentally are much closer to the situation where no O is stored at the oxide/metal interface.

For the O-vacancies, we include in Table II the average *z* position for the layer without the cation closer to the vacancy, that usually shows different features, and the *z* position of the Mg cation directly in contact with the vacancy. Also, lateral displacements for the Mg cations first neighbors to the vacancy are reported. The most striking point in Table II is the extraction of the Ag atom out of the topmost Ag layer by 0.2–0.3 Å occurring when the O vacancy is present at the oxide/metal interface. Extraction of the Ag atom is not observed if the vacancy is present at the surface of a 2 ML deposit. The corrugation observed in the regular film is in-

TABLE II. Geometries for monolayer and bilayer of MgO adsorbed on Ag(001) in a $p(2\times2)$ supercell for an O-related defect. Coordinates and displacements are in Å. d_{Mg} stands for the lateral displacement of Mg atoms first near neighbors to the vacancy and $\overline{z}$ stands for the average for the rest of Ag or Mg atoms in the plane not directly in contact with the defect. *Oi* stands for the MgO/O/Ag system, *Vi* for the MgO film containing a vacancy at the interface and *Vs* for the system containing a vacancy at the surface. $L=1$ and 2 indicate the number of MgO layers in the film.

L	$\overline{z}_{Ag}$	z_{Oi}	z_{Os}	z_{Mgs}	$\overline{z}_{Mgs}$				
Oi 1	0.013	0.482	2.727	2.478	2.727				
L	z_{Ag}	$\overline{z}_{Ag}$	z_{Oi}	z_{Mgi}	$\overline{z}_{Mgi}$	d_{Mg}	z_{Os}	z_{Mgs}	$\overline{z}Mgs$
Vis 1	0.307	−0.050	2.650	-	2.399	−0.066	-	-	-
Vi 2	0.202	−0.102	2.536	-	2.388	0.000	4.703	4.833	4.634
Vs 2	-	−0.010	2.824	2.343	2.713	0.052	5.005	-	4.928

creased when vacancies are present, due to the induced corrugation in the O-sublattice. For instance, for 1 ML, anion-cation corrugation is at least 0.13 Å, but also the O-sublattice shows an almost 0.2 Å difference in the oxygen vertical displacements. Again, when two monolayers are considered, the anion-cation distance in the *z*-direction is reduced to less than 0.08 Å and the O-sublattice is almost coplanar. For the bilayer, when the vacancy is present at the interface the highest point on the surface is the Mg atom on top of the vacancy, 0.2 Å higher than the rest of Mg atoms in the surface layer; even higher than O in this layer. A final feature is the lateral displacement of the Mg cations neighboring a vacancy. For the bulk and surface unsupported MgO, lateral displacements always give more space for the two electrons in the vacancy, indicating that Mg atoms are pushed out of the center of the vacancy. In the present model this feature is only seen for a surface vacancy at the bilayer. The lack of lateral displacements in the resting structures is therefore due to the presence of Ag.

B. Energetics at the interface

Binding energies for MgO on Ag(001), shown in Table III, are very low for nondefective films, about 0.36 eV for a single monolayer and 0.19 eV for the bilayer, with respect to a MgO unit in contact with the surface and within the PW91 approach, which is known to give rise to overbinding.[35] These energies, relative to the MgO unit are quite small, in agreement with the low interaction found for the reversed system through microcalorimetric experiments. For large Ag islands on MgO a binding energy of 15 kJ/mol was found.[36] The lowest binding energy obtained for a bilayer is a consequence of reduction in the extent of relaxation and the consequent energy gain. The stiffness of the structure, a characteristic of ionic oxides, is retrieved for the bilayer, reducing the relaxation of the structure. This reduction of the relaxation might be relevant when considering larger deposits. Moreover, since the bond at the interface is relatively weak compared to the cohesive energy of the MgO, deposits will try to grow tridimensionally, as has been seen experimentally.[9]

The binding energy of O_2 to the Ag(001) for low coverages, 0.25 ML, and with respect to O_2 and the Ag slab is 0.86 eV per oxygen atom. This is the most stable situation for this coverage since subsurface O structures are higher in energy by more than 1.5 eV/atom. This preoxidized structure binds the MgO monolayer by 1.6 eV. According to these values it cannot be discarded that if an excess of O_2 is present in the preparations some O can be stored at the interface in a binary Mg, Ag oxide form. Moreover, these structures are stable against the formation of O_2 and a vacancy at the film by more than 5 eV.

Considering now the oxygen poor condition, O-vacancies can be present in the oxide film. To form an oxygen vacancy in the MgO film costs about 5.43 eV with respect to gas phase oxygen for a single monolayer and 6.71 eV for the bilayer. When adsorbing these defective films to the Ag(001) substrate the binding energies of the defective oxide film to the metal are larger than for the regular film, around 2 eV/defect when the vacancy is at the interface and 1.7 eV when the vacancy is on the topmost layer. In this case the energy increases for 2 ML if the vacancy is at the interface. As for metals on oxides, vacancies on the oxide layer favor the intermetallic bond formation, a much more effective bonding mechanism than the polarization of the metal induced by the presence of the oxide. In fact, the bond when vacancies are present is much stronger since electrons kept in the cavity can be shared between the oxide layer and the substrate. For the bilayer, the relatively large difference, 0.5 eV, between the position of the vacancy on the surface layer and at the interface indicates that the interface behaves as a sink for this kind of defect. Vacancy diffusion is likely to be easier for very small structures (2 ML deposited) than for larger structures (3 ML deposited) due to the reduction in the coordination number. For a 3 ML deposit, diffusion would resemble that in the bulk, which has been determined to show energy barriers of about 3.5 eV.[37,38]

C. Electronic structure

The analysis of the electronic structure for the oxide supported on the metal is performed through the projected local density of states, LDOS, determined for all the systems considered. Partial LDOS are reported in Fig. 2 for the surface Ag, O and Mg atoms. To illustrate the chemical changes a deep zoom on the region near the Fermi level is shown. For the complex $p(2\times2)$ structures symmetry can break and different lines corresponding to nonequivalent species have been drawn in Fig. 2. The plots for the electronic structures shown here are somehow different than those of Ref. 9 in the sense that the total density of states has been split into the atoms by projecting the total density on the atomic orbitals up to a given radius. The projected density of states provides a clue to understand the origin of corrugation in STM images since it separates the contributions from the different atoms present. However, since Mg(3*sp*) states are very extended in nature, the projections do not include all the empty states that correspond to these atoms. We have done comparisons employing a larger radius in the projection, 2 vs. 1 bohr. The results show that all cases the conduction band is mainly of Mg(3*sp*) character and its position depends on the nature of the system. The main drawback when employing a larger radius in the projection of the states into the atoms is that it leads to double counting, by artificially assigning twice the electronic density located at the interstitial regions.

Besides this aspect, plots for the regular systems are very similar to results in Ref. 9; see Figs. 2(a) and 2(b). The MgO to Ag bond for the undefected film is mainly formed by metal polarization, as previously seen for the metal/oxide counterpart.[39] The valence band is mainly of O(2*p*) origin and at the Fermi level only Ag and O states are present.

For nonstoichiometric systems, the electronic structure is modified to different extents. A large perturbation occurs for the preoxidized Ag system; see Fig. 2(e). In this case, the Ag and the O_i states show significant covalent contributions and a corresponding modification of the Ag related band with both bonding and antibonding states. This shows the highly covalent character of the Ag-O bonding compared to the

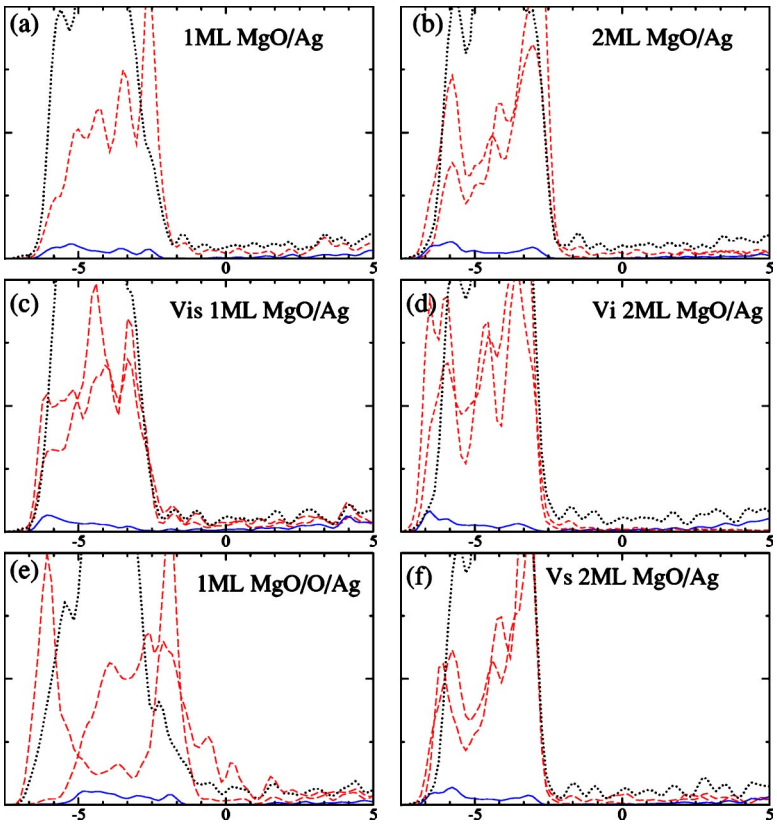

FIG. 2. (Color online) Projected local density of states for MgO/Ag systems. Dotted lines state for Ag, dashed lines for O and continuous lines for Mg. The top panel shows stoichiometric deposits: left 1 ML MgO/Ag, right 2 ML MgO/Ag. The central panel shows deposits with vacancies at the MgO/Ag interface: left 1 ML, right 2 ML. The bottom panel shows the following: left, MgO/O/Ag structure and right, surface oxygen vacancy at 2 ML MgO/Ag. Zero energy in the *x*-axis corresponds to the Fermi level.

charge polarization occuring for the regular MgO-Ag interaction where the Ag interacts directly with O^{2-} anions in the MgO layer.

The LDOS for the defective O structures is shown in Figs. 2(c) and 2(d) and 2(f). If the vacancy is present at the interface between MgO and Ag, the Ag atom in direct contact to the vacancy gets some charge by the two electrons left in the vacancy. A similar phenomenum has been described by Giordano and co. for both the MgO/Pd(001) interface and the reversed Pd/MgO(001) systems.[40,41] If the vacancy is present at the interface, the Mg atoms also modify their structure contributing to the bond at the interface, thus resembling an intermetallic bond. When the vacancy is present at the surface, Fig. 2(f), the LDOS is similar to that of the oxide slab alone. Again, due to the projection employed to obtain the LDOS the vacancy or impurity level in the gap of MgO is difficult to detect. However, the vacancy related features can be retrieved with the density analysis performed through the simulation of the STM images, as we will show in the next section.

D. STM: Calculated images

Calculated STM images have been generated for zero and positive bias (tunnelling from the tip to the substrate). In all the figures a $p(2\times2)$ cell is employed to understand the position of the areas with larger tunnelling currents. They can be compared to the STM experiments by the groups of Schneider[9] and Valeri[26] that reach atomic resolution on these films.

The contrast in the images obtained in STM have two different origins: the electronic structure and the geometric structure. Depending on the conditions of the film and on the presence and quality of the defects their fingerprints at different voltages can be characteristic.

The origin of the contrast for the regular films is revealed in the first images, Fig. 3. For regular surfaces the contrast at zero bias is completely governed by the Ag states at the Fermi level. When increasing the bias a series of empty states, also more extended into the vacuum, are available for tunnelling. These states come from the conduction band of the supported oxide mainly located at the Mg positions. The resulting competition between both gives rise to a change in the corrugation: protrusions at 0 and positive voltages are placed in different positions for the monolayer, where Ag and Mg atoms are alternated. For the adsorbed bilayer, where both Ag and surface Mg sit on the same position in the plane, the initial image is conserved on going to higher voltages. The present simulations confirm the suggestions[9] about the double origin of the tunnelling at low and high voltages and assign unequivocally that Mg atoms are imaged at high voltages for regular surfaces. This assignment can only be done by comparing simulated images to the observed STM ones. Care must be taken since the tendency of PW91 to underestimate the band gap for insulators is well known.[42] This could lead to differences for the quantitative comparison between the simulated images presented here and those reported in the experiments. However, it does not affect the qualitative description or the assignment of the centers responsible for tunnelling.

Images corresponding to the preoxidized Ag system are presented in Fig. 4. The image for the complex MgO/O/Ag(001) $p(2\times2)$ has the origin of contrasts in a complex mixture of geometrical and electronic factors. Due

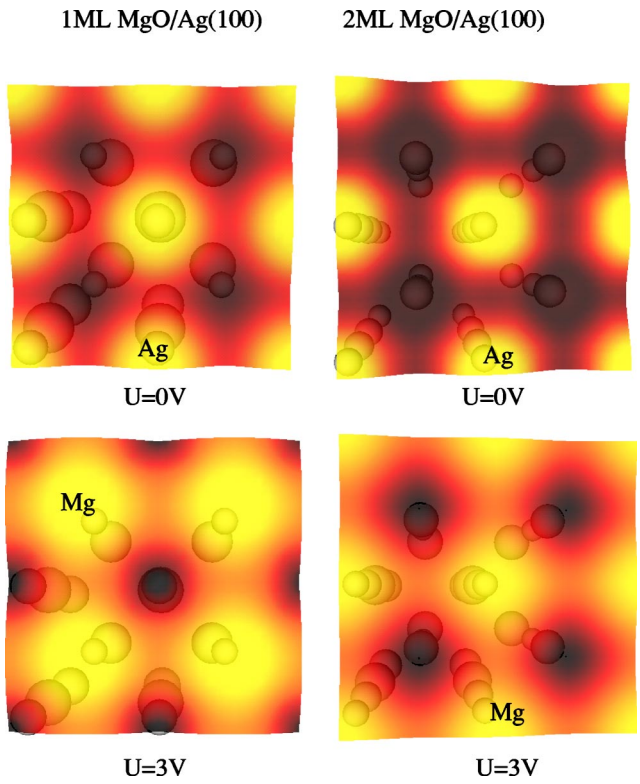

FIG. 3. (Color online) Simulated STM images for MgO on Ag(001) revealing the origin of the contrast for the same structure at different voltages ranging from 0 (Ag atoms images) to a positive 3 Volt value (Mg atoms are observed). On the left panels 1 ML regular MgO is considered while 2 ML deposits are shown on the right column.

to the presence of O, Ag atoms are not as prone for tunnelling as for the regular regions; see Fig. 2. Moreover the distances from Ag to the tip are enlarged due to the thicker amplitude of the MgO insulator film. The corrugation observed at 0 V shows two of the Mg atoms, the ones located at larger distances from the substrate, while the one on the top corner which is place 0.1 Å lower is seen as a dark area due to the increase in the distance from the tip. The Mg atom in contact with the interstitial O is not particularly dark even if it is placed much lower than the Mg on the top corner; this is due to the fact that the underlying O atoms have a significant density at the Fermi level; see Fig. 2. These electronic contributions partially compensate those coming from the geometry, e.g., the lower position of the Mg atom. At positive larger voltages the image is partially reversed, the bright Mg centers are even brighter but the position where the interstitial O atom is located are seen as dark areas. This is due to the amount of contributions from the empty states of the Mg atoms that in this case only reproduce the geometrical structure found.

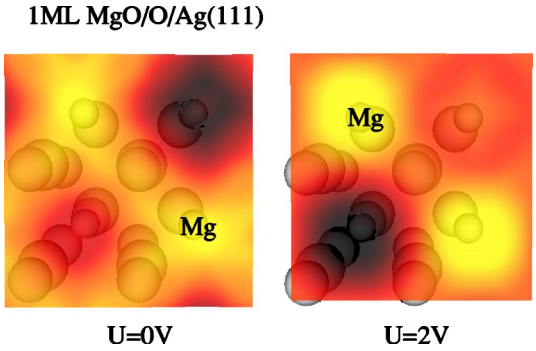

FIG. 4. (Color online) Simulated STM images for the MgO/O/Ag(001) system. Images shown correspond to 0 and 2 Volt voltages.

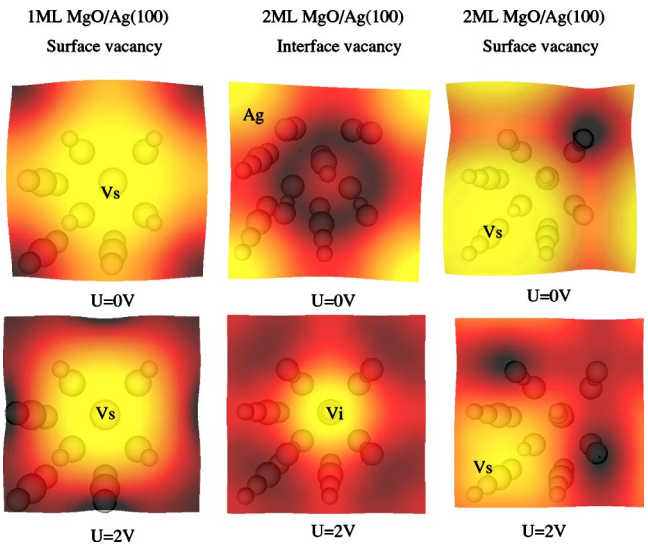

FIG. 5. (Color online) Simulated STM images for defective MgO layers on Ag(001), first column 1 ML MgO, second and third columns 2 ML of MgO with the vacancies in different positions.

When vacancies are present at the surface oxide layers, Fig. 5, they are mainly seen as protrusions and they are stable in the image from zero to positive large voltages. This is seen when the defect is located in the surface; see the columns on the left and right in Fig. 5. In that case, vacancies completely control the shape of the image. As found for rutile $TiO_2(110)$ the extension of the vacancy-related features is much larger than those corresponding to Ag or Mg atoms. If the defect is present at the interface between a bilayer of MgO and Ag the image at low bias seems to be determined by the Ag states close to the Fermi level. In that case, at zero voltage, a big depression at the position of the vacancy is seen. However, at positive voltages a bright protrusion is present at the same position although in that case the extension is smaller than that found when the vacancy is present in the topmost layer. The observed corrugation in this case is due to geometrical effects. Tunnelling is, as before, controlled by the Ag states at low voltages while it is due to empty Mg states at positive voltages. However, looking at Table III, the Mg atom on top of the vacancy site is out of the MgO plane by 0.2 Å. At zero voltage, the distance for tunnelling between the tip and the Ag atom directly below the vacancy site is much larger than for other Ag positions, resulting in a lower current from this position. The contrary holds at high voltages where the Mg center on top of the vacancy has a maximum intensity because it is slightly out from the plane of the second layer of Mg atoms resulting in a larger tunnelling from this position.

TABLE III. Binding energy in eV per MgO unit or per O-defect when these defects are present. The energies are calculated with respect to the MgO film, or defective film. For the O-excess system the energy is calculated with respect to the oxygen precovered silver surface. See the text for a further discussion.

System	1 ML	2 ML	1 ML *Oi*	1 ML *Vis*	2 ML *Vs*	2 ML *Vi*
BE	0.36	0.19	1.57	2.08	1.65	2.23

IV. CONCLUSIONS

We have performed DFT slab calculations on the MgO/Ag(001) system considering one and two layers of MgO. For the regular, stoichiometric, system corrugation of a single MgO layer is observed while the stiffer bilayer prevents this energy release mechanism. The consequence is that the binding energy of the oxide to the metal already small, 0.3 eV, for the monolayer, (the bonding is based in polarization effects) is further reduced for the bilayer, aproximately 0.2 eV. Nonstochiometric conditions generate two different structures. O-deficient conditions favor the bond at the interface by a very large amount, about 2 eV. This value is reduced if the vacancy instead of being at the interface layer is placed at the surface layer. In excess oxygen, the bond at the partially oxidized interface is also larger than for the clean Ag(001). Geometries are also changed in both excess and deficiency limits. The electronic structure of deposits changes strongly in out-stoichiometric conditions, by modifying the shape and positions of some of the bands.

For the STM images, we can conclude the following: at low voltages and provided than the film is thin enough Ag states are responsible for the contrast found, but when the voltage is increased Mg cations on the surface are the responsibles for tunnelling. It is possible then to obtain a reverse picture by changing the voltage applied from zero to positive values depending on the number of MgO layers in the deposit. If vacancies are present on the topmost layer of the film, they are imaged as protrusions and dominate the images. But if vacancies are at the interface big protrusions are observed only at positive voltages. Finally, interficial O atoms are present they are seen as black areas in the images at positive voltages.

ACKNOWLEDGMENTS

The authors are grateful to G. Pacchioni, L. Giordano, M. Trioni, Z. Lodziana, and F. Illas for useful discussions. Financial support comes from the Spanish Ministry of Science and Technology through the Ramon y Cajal program and the BQU2002-04029-CO2-01 project. CEPBA is acknowledged for a generous time allocation and O. H. Nielsen and L. B. Hansen for their help with the DACAPO code.

[1] C. R. Henry, Surf. Sci. Rep. **31**, 231 (1998).
[2] C. T. Campbell, Surf. Sci. Rep. **227**, 1 (1997).
[3] P. L. Hansen, J. B. Wagner, S. Helveg, J. R. Rostrup-Nielsen, B. S. Clausen, and H. Topsøe, Science **295**, 2053 (2002).
[4] E. A. A. Jarvis, A. Christensen, and E. A. Carter, Surf. Sci. **487**, 55 (2001).
[5] E. Lundgren, G. Kresse, C. Klein, M. Borg, J. N. Andersen, M. De Santis, Y. Gauthier, C. Konvicka, M. Schmid, and P. Varga, Phys. Rev. Lett. **88**, 246103 (2002).
[6] D. W. Goodman, J. Catal. **216**, 213 (2003).
[7] K. H. Hansen, T. Worren, S. Stempel, E. Laegsgaard, M. Baumer, H.-J. Freund, F. Besenbacher, and I. Stensgaard, Phys. Rev. Lett. **83**, 4120 (1999).
[8] D. R. Jennison, C. Verdozzi, P. A. Schultz, and M. P. Sears, Phys. Rev. B **59**, R15 605 (1999).
[9] S. Schintke, S. Messerli, M. Pivetta, F. Patthey, L. Libioulle, M. Stengel, A. De Vita, and W.-D. Schneider, Phys. Rev. Lett. **87**, 276801 (2001).
[10] S. Schintke and W.-D. Schneider, J. Phys.: Condens. Matter **16**, R49 (2004).
[11] S. Altieri, L. H. Theng, F. C. Voogt, T. Hibma, O. Rogjanu, and G. A. Sawatzky, Phys. Rev. B **66**, 155432 (2002).
[12] S. Altieri, L. H. Tjeng, and G. A. Sawatzky, Phys. Rev. B **61**, 16 948 (2000).
[13] J. Goniakowski, Phys. Rev. B **59**, 11 047 (1999).
[14] Yu. F. Zhukovskii, E. A. Kotomin, P. W. M. Jacobs, and A. M. Stoneham, Phys. Rev. Lett. **84**, 1256 (2000).
[15] J. R. Smith, T. Hong, and D. J. Srolovitz, Phys. Rev. Lett. **72**, 4021 (1994).
[16] M. Sgroi, C. Pisani, and M. Busso, Thin Solid Films **400**, 64 (2001).
[17] C. Lamberti, E. Groppo, C. Prestipino, S. Casassa, A. M. Ferrari, C. Pisani, C. Giovanardi, P. Luches, S. Valeri, and F. Boscherini, Phys. Rev. Lett. **91**, 046101 (2003).
[18] http://www.fysik.dtu.dk/CAMPOS
[19] D. H. Vanderbilt, Phys. Rev. B **41**, 7892 (1990).
[20] J. P. Perdew *et al.* Phys. Rev. B **46**, 6671 (1992); J. A. White and D. M. Bird, *ibid.* **50**, 4954 (1994).
[21] G. Kresse and J. Forthmüller, Comput. Mater. Sci. **6**, 15 (1996).
[22] P. Bloechl, G. P. Das, H. F. Fischmeister, and U. Schoenberger, *Proceedings of the International Workshop*, Metal-Ceramic Interfaces, Santa Barbara, CA, 16–18 January 1989; M. Ruehle, A. G. Evans, M. F. Ashby, and J. P. Hirth, Acta Metallurgica, Inc., 1990, pp. 9–14.
[23] S. Valeri, S. Altieri, A. Di Bona, C. Giovanardi, and T. S. Moia, Thin Solid Films **400**, 16 (2001).
[24] M. Teodorova, W. X. Li, M. V. Ganduglia-Pirovano, C. Stampfl, K. Reuter, and M. Scheffler, Phys. Rev. Lett. **89**, 096103 (2002).
[25] J. Tersoff and D. R. Hamann, Phys. Rev. Lett. **50**, 1998 (1983).
[26] S. Valeri, S. Altieri, U. del Pennino, A. di Bona, P. Luches, and A. Rota, Phys. Rev. B **65**, 245410 (2002).
[27] U. Diebold, J. F. Anderson, K.-O. Ng, and D. Vanderbilt, Phys. Rev. Lett. **77**, 1322 (1996).
[28] K.-O. Ng and D. Vanderbilt, Phys. Rev. B **56**, 10 544 (1997).
[29] R. Schaub, P. Thostrup, N. Lopez, E. Laegsgaard, I. Stengsgaard,

J. K. Nørskov, and F. Besenbacher, Phys. Rev. Lett. **87**, 266104 (2001).
[30] J. Cerda, M. A. Van Hove, P. Sautet, and M. Salmeron, Phys. Rev. B **56**, 15 885 (1997).
[31] C. Giovanardi, A. Di Bona, T. S. Moia, S. Valeri, C. Pisani, M. Sgroi, and M. Busso, Surf. Sci. **505**, L209 (2002).
[32] A. M. Flank, R. Delaunay, P. Lagarde, M. Pompa, and J. Jupille, Phys. Rev. B **53**, R1737 (1996).
[33] S. Valeri, S. Altieri, A. Di Bona, P. Luches, G. Giovardi, and T. S. Moia, Surf. Sci. **507–510**, 311 (2002).
[34] M. Rocca, L. Savio, L. Vattuone, U. Burghaus, V. Palomba, N. Novelli, F. Buatier de Mongeot, U. Valbusa, R. Gunnella, G. Comelli, A. Baraldi, S. Lizzit, and G. Paolucci, Phys. Rev. B **61**, 213 (2000).
[35] B. Hammer, L. B. Hansen, and J. K. Nørskov, Phys. Rev. B **59**, 7413 (1999).
[36] J. H. Larsen, J. T. Ranney, D. E. Starr, J. E. Musgrove, and C. T. Campbell, Phys. Rev. B **63**, 195410 (2001).
[37] V. N. Kuzokov, A. I. Popov, E. A. Kotomin, M. A. Monge, R. Gonzalez, and Y. Chen, Phys. Rev. B **64**, 064102 (2001).
[38] J. Carrasco, N. Lopez, and F. Illas (submitted).
[39] I. Yudanov, G. Pacchioni, K. Neyman, and N. Rosch, J. Phys. Chem. B **101**, 2786 (1997).
[40] L. Giordano, J. Goniakowski, and G. Pacchioni, Phys. Rev. B **67**, 045410 (2003).
[41] L. Giordano, J. Goniakowski, and G. Pacchioni, Phys. Rev. B **64**, 075417 (2001).
[42] I. de P. R. Moreira, F. Illas, and R. L. Martin, Phys. Rev. B **65**, 155102 (2002).